Observational Study

Medicine

OPEN

The prognostic value and immunological role of calcium/calmodulin dependent protein kinase kinase 2 (*CAMKK2*) in pan-cancer study

Senjun Jin, MD[a], Yanyan Wang, MD[b], Sheng'an Hu, MD[a], Guangzhao Yan, MD[a,*]

Abstract

A thorough assessment of calcium/calmodulin dependent protein kinase kinase 2 (*CAMKK2*) in pan-cancer studies is currently absent. We integrate multi-omics and clinical data to conduct a molecular landscape of *CAMKK2*. Gene variation results revealed abnormal high frequency mutations of *CAMKK2* in uterine corpus endometrial carcinoma, while expression level analysis demonstrated relatively high expression of *CAMKK2* in prostate adenocarcinoma. The aberrant expression of *CAMKK2* was found to be predictive of survival outcomes in several cancer types. Additionally, we identified potential regulators of *CAMKK2* expression, including miRNAs such as miR.129.1.3p, as well as small-molecule drugs such as EPZ004777, which significantly correlated with *CAMKK2* expression. Single-cell transcriptome analysis of kidney renal clear cell carcinoma further revealed a significantly higher expression of *CAMKK2* in and monocyte and macrophage M1. Furthermore, in the kidney renal clear cell carcinoma IMvigor210 cohort, patients ongoing immunotherapy with higher *CAMKK2* expression experienced a significantly longer median overall survival, but it was observed that in bladder urothelial carcinoma GSE176307 and skin cutaneous melanoma GSE78220 cohorts, *CAMKK2* might significantly prolong overall survival. Briefly, *CAMKK2* emerges as a promising molecular biomarker that holds potential implications for prognostic evaluation and predicting the effectiveness of immunotherapy across cancers.

Abbreviations: BLCA = bladder urothelial carcinoma, BRCA = breast invasive carcinoma, CAMKK2 = calcium/calmodulin dependent protein kinase kinase 2, CNV = copy number variations, GEO = Gene Expression Omnibus, HPA = Human Protein Atlas, HR = hazard ratios, KIRC = kidney renal clear cell carcinoma, KM = Kaplan–Meier, LGG = lower grade glioma, LIHC = liver hepatocellular carcinoma, LUSC = lung squamous cell carcinoma, MESO = mesothelioma, NK = natural killer, OS = overall survival, OV = ovarian serous cystadenocarcinoma, PRAD = prostate adenocarcinoma, SKCM = skin cutaneous melanoma, STAD = stomach adenocarcinoma, TCGA = The Cancer Genome Atlas, THCA = thyroid carcinoma, UCEC = uterine corpus endometrial carcinoma, UVM = uveal melanoma.

Keywords: *CAMKK2*, immunotherapy, pan-cancer, prognosis

1. Introduction

Cancer has emerged as the second most prominent cause of global mortality, trailing only cardiovascular disease.[1] According to the latest epidemiological studies, approximately 18 million individuals worldwide received new cancer diagnoses in 2018, and predictive models indicate an overall risk of 20.2% for developing cancer in the age range of 0 to 74 years.[2] Despite some advancements in controlling the overall mortality rate through research on cancer pathogenesis and treatments over the last 2 decades, a comprehensive understanding of its biological characteristics has not yet met the criteria of precision medicine.[3,4] The tumor's resilience to inhibitory responses within the pathways responsible for cancer hallmarks is attributed to genomic mutations and epigenetic alterations.[5] As clinical drug development increasingly relies on gene mutations and kinase inhibition, there is a growing demand for in-depth investigations into the molecular mechanisms of tumors. Furthermore, exploring tumor immunity through in vivo and in vitro studies has highlighted the urgent necessity of identifying additional biomarkers to aid in the diagnosis and prognosis of cancer.

SJ and YW contributed equally to this work.

This work was supported by Clinical Research Project of Zhejiang Provincial Administration of Traditional Chinese Medicine (2023ZL253).

The authors have no conflicts of interest to disclose.

The datasets generated during and/or analyzed during the current study are publicly available.

[a] Department of Emergency Medicine, Emergency and Critical Care Center, Zhejiang Provincial People's Hospital, Affiliated People's Hospital, Hangzhou Medical College, Hangzhou, Zhejiang, China, [b] Department of Clinical Laboratory, Laboratory Medicine Center, Zhejiang Provincial People's Hospital, Affiliated People's Hospital, Hangzhou Medical College, Hangzhou, Zhejiang, China.

** Correspondence: Guangzhao Yan, Department of Emergency Medicine, Emergency and Critical Care Center, Zhejiang Provincial People's Hospital, Affiliated People's Hospital, Hangzhou Medical College, Hangzhou, Zhejiang, 310014, China (e-mail: ygz3362429@hotmail.com).*

How to cite this article: Jin S, Wang Y, Hu S, Yan G. The prognostic value and immunological role of calcium/calmodulin dependent protein kinase kinase 2 (CAMKK2) in pan-cancer study. Medicine 2024;103:41(e40072).

Received: 4 February 2024 / Received in final form: 20 September 2024 / Accepted: 25 September 2024

http://dx.doi.org/10.1097/MD.0000000000040072

The calcium/calmodulin dependent protein kinase kinase 2 (*CAMKK2*) gene locus, spanning over 40 kb pairs, is situated on chromosome 12q24.2 and comprises 18 exons and 17 introns.[6] Like other members of the calmodulin kinase family, *CAMKK2* exhibits distinct N- and C-terminal domains, alongside a central Ser/Thr-directed kinase domain, followed by a regulatory domain consisting of overlapping autoinhibitory and calmodulin-binding regions.[7] Isoform variability primarily arises from differences in the carboxy termini, resulting in the existence of 7 *CAMKK2* isoforms generated through alternative splicing and/or variable utilization of polyadenylation sites.[6,8] Isoform 1 of *CAMKK2* is the most abundantly expressed isoform, particularly in the brain and throughout the body.[6] Initially, *CAMKK2* was found to regulate memory formation, long-term memory, and appetite through the activation of cAMP-responsive elements in the hippocampus.[6,9] While isoform 2 of *CAMKK2* is expressed in several brain cancer cell lines, it is the predominant isoform in the prostate, regardless of the presence of cancer.[10] Subsequent studies have demonstrated that *CAMKK2* serves as a direct androgen receptor-target gene and functional driver of prostate cancer progression.[8,10,11] Moreover, higher *CAMKK2* activity has been associated with tumor aggravation in various cancer cell lines, including glioblastoma multiforme, liver hepatocellular carcinoma (LIHC), ovarian serous cystadenocarcinoma (OV), and stomach adenocarcinoma (STAD).[12–14] Despite the significant importance of *CAMKK2*, there is currently a lack of public resources providing prognostic information on *CAMKK2* in a broader range of cancer types.

In addition to its expression in tumor cells, *CAMKK2* is also found in various immune cells, including macrophages, myeloid cells, myeloid-derived suppressor cells (MDSCs), and natural killer (NK) cells.[15–18] *CAMKK2* expression in macrophages and myeloid cells has been associated with decreased recruitment of T cells.[15,16] Interestingly, intrinsic deletion of *CAMKK2* in MDSCs and NK cells surprisingly leads to increased metastatic progression, highlighting a crucial role for this enzyme in the antitumor immune response.[17,18] However, the precise molecular mechanisms underlying the opposing functions of *CAMKK2* in different immune cells require further investigation.

In the present study, we employed a combination of The Cancer Genome Atlas (TCGA) project and Gene Expression Omnibus (GEO) databases to perform a comprehensive pan-cancer analysis of *CAMKK2*. Our analysis encompassed various aspects, including the assessment of genetic alterations, differential expression patterns, subcellular localization, correlations with patient survival, identification of associated microRNAs, and exploration of potential drug candidates. Moreover, we investigated that *CAMKK2* served as a biomarker to predict immunotherapy response in 6 real-world immunotherapy cohorts and 2 single-cell datasets. To the best of our knowledge, this study represents the first extensive analysis of *CAMKK2*'s molecular mechanisms in pan-cancer using multi-omics data.

2. Materials and methods

2.1. Data acquisition

Transcriptomic profiles and paired overall survival (OS) outcome, copy number variations (CNVs), single-nucleotide polymorphisms of 33 cancer types from TCGA was downloaded from https://xenabrowser.net/datapages/. Data from 3 immunotherapy cohorts (bladder urothelial carcinoma [BLCA] GSE176307; skin cutaneous melanoma [SKCM] GSE78220, and SKCM GSE91061) were downloaded from GEO.[19–21] Data from other 3 immunotherapy cohorts (BLCA, IMvigor210; kidney renal clear cell carcinoma (KIRC) IMvigor210; KIRC PMID32472114) were downloaded from supplementary materials of the 2 literatures.[22,23] Two single-cell datasets of KIRC, GSE139555, and GSE145281, were downloaded from GEO.[24,25]

2.2. CAMKK2 genomic variant

We collected a comprehensive cohort of 11,124 patients to determine the prevalence of *CAMKK2* mutations, CNV amplification, and deep deletion. The number of patients with *CAMKK2* genetic variants was shown in the bar plot by the R package ggpubr.[26] The alteration ratio of *CAMKK2* in each cancer type was calculated as the percentage of abnormal genomic variants relative to all tumors associated with that specific cancer. The percent of alteration ratio was generated in a heatmap by the R package pheatmap.[27] To evaluate the impact of *CAMKK2* variants on patient outcomes, we analyzed survival data using Kaplan–Meier (KM) curves via the R packages "survminer" and "survival," including log-rank P value < .05, median overall survival (mOS), and hazard ratios (HR).[28,29]

2.3. The mRNA expression of CAMKK2

We collected the TPM (transcripts per million) values of *CAMKK2* mRNA from the transcriptomic profiles in pan-cancer. To ensure robustness and account for potential batch effects, data from different test batches were averaged. Additional information on the GDC (Genomic Data Commons) pipeline can be found on their website at https://docs.gdc.cancer.gov. For statistical validity, we focused on sixteen cancer types that had more than 10 paired normal samples available. These cancers were included in the comparative analysis of differential expression between tumor tissues and their respective normal tissues. Differences between groups were accomplished by Wilcoxon test with P value < .05 in the R package ggpubr.[26]

2.4. Immunohistochemistry and immunofluorescence

For the experiments involving immunohistochemistry and immunofluorescence, we utilized the *CAMKK2* antibodies HPA017389 and HPA063713 obtained from Sigma-Aldrich. All experimental results have been meticulously conducted and documented in the Human Protein Atlas (HPA),[30] which can be accessed at https://www.proteinatlas.org/. In the immunohistochemistry experiments, tumor and normal tissue samples were collected from various organs in the HPA, including the breast, colon, lung, prostate, and kidney (https://www.proteinatlas.org/ENSG00000110931-CAMKK2/pathology). These samples were then subjected to immunohistochemical staining using the *CAMKK2* antibodies. In addition, 3 different cell lines, namely A-431, U-251MG, and U2OS, were utilized for the immunofluorescence experiments in the HPA (https://www.proteinatlas.org/ENSG00000110931-CAMKK2/subcellular#human).[30] These cell lines were treated with the *CAMKK2* antibodies to investigate the subcellular localization and distribution of *CAMKK2* protein. Detailed experimental methods have been described at https://www.proteinatlas.org/about/assays+annotation. All these experimental results, including immunohistochemistry and immunofluorescence findings, can be accessed and explored in detail on the HPA website.[30]

2.5. Overall survival outcome

Survival analysis of patients was carried out using the R package survival. To determine the optimal cutoff value for continuous *CAMKK2* expression, we utilized the surv_cutpoint function via the R packages "survival" to categorize patients into 2 groups with high and low CAMKK2 expression.[28] Subsequently, a correlation analysis between *CAMKK2* expression levels (divided into high and low groups) and overall survival was performed. For visualization purposes, forest plots and KM plots were generated using the R packages forestplot and survminer, respectively.[29,31] The forest plot provided a graphical representation

of the HR and 95% confidence intervals, while the KM plots displayed the survival curves for patients in the *CAMKK2* high and low expression groups.

2.6. CAMKK2-targeted miRNA

To predict miRNA candidates targeting *CAMKK2*, we utilized the R package multiMiR,[32] which incorporates 7 miRNA–mRNA link databases, namely ElMMo, MicroCosm, miRanda, DIANA-microT, PITA, and TargetScan. These databases were used to identify potential miRNA binding sites within the *CAMKK2* mRNA sequence. The prediction results obtained from these databases were visualized using the R package UpSetR, which allows for the creation of an upset map.[33] This map provides a comprehensive overview of the shared and unique miRNA predictions across the different databases. These miRNAs that are simultaneously predicted to target CAMKK2 by 3 different databases deserve more attention. To further analyze the relationship between *CAMKK2* and the predicted miRNAs, we calculated the Pearson correlation coefficient with P value < .05 using the R package Hmisc.[34] This correlation analysis provides insights into the potential regulatory associations between *CAMKK2* and the identified miRNAs. The resulting correlation values were then visualized using the R package pheatmap, generating a heatmap representation.[27]

2.7. Drug sensitivity

The Genomics of Drug Sensitivity in Cancer version 2 database provides valuable information on IC50 values and transcriptomic data for 167 cell lines treated with various drugs. To analyze the correlation between drug sensitivity and *CAMKK2* expression, we utilized the R package oncoPredict.[35] This package enables the prediction of drug IC50 values for each patient in the TCGA dataset based on their transcriptomic data. To investigate the relationship between IC50 values and *CAMKK2* expression, we calculated the Pearson correlation coefficient. This analysis assessed the strength and direction of the correlation between drug sensitivity and *CAMKK2* expression levels. For visual representation, we generated a heatmap, scatter plot, and box plot.[26] These plots provide insights into the relationship between drug sensitivity and *CAMKK2* expression. The scatter plot was specifically created using the R package ggpubr, which offers customizable and visually appealing scatter plots.[26]

2.8. Single-cell distribution

The analysis of 2 single-cell datasets of KIRC, namely GSE139555 and GSE145281, was conducted using the online platform Tumor Immune Single-cell Hub (TISCH).[24,25,36] To ensure data quality, low-quality cells were filtered out based on 2 criteria: cells with a total count <1000 and cells with a number of detected genes <500. Both datasets were then uniformly processed using the MAESTRO workflow.[37] Furthermore, to address potential batch effects, datasets with a median entropy lower than 0.7 underwent batch correction using the R package Seurat.[38] This step helped to minimize any technical variations between the datasets and ensured more reliable downstream analyses. In the analysis, cell markers, such as CD80, which serves as a marker for macrophage M2, were obtained from the CellMarker 2.0 database (http://bio-bigdata.hrbmu.edu.cn/CellMarker).[39] These cell markers played a crucial role in identifying and characterizing specific cell types within the KIRC single-cell datasets.

2.9. Immunotherapy outcome

Six cohorts with patients receiving immunotherapy, including transcriptomic profiles and clinical information were collected as described in Section 2.1. Survival analysis of patients with various *CAMKK2* expression was referred to the Section 2.5 in the present study. This analysis involved stratifying patients based on their *CAMKK2* expression levels and comparing their survival outcomes via the R packages "survminer and "survival."[28,29] By examining the relationship between *CAMKK2* expression and overall survival, the study aimed to elucidate the potential prognostic value of *CAMKK2* in the context of immunotherapy.

2.10. Statistical analysis

The statistical analysis was conducted using the R program within the RStudio platform.[40,41] For comparing differences between 2 groups, the default Wilcoxon test was employed. On the other hand, when comparing differences among multiple groups, a one-way analysis of variance (ANOVA) was performed. To assess the impact of different factors on overall survival, KM analysis and a log-rank test were utilized. These methods allowed for the comparison of survival curves between different groups. In all statistical analyses, a significance level of $P < .05$ was considered statistically significant unless otherwise specified. This threshold was used to determine the presence of significant differences or associations between variables under investigation.

2.11. Ethical statement

All the data used in this study was open-access data from online databases, so the ethical approval was not necessary in our research.

3. Result

3.1. Study design

Our study consists of 6 main steps, namely data collection, mutated CAMKK2, altered CAMKK2 expression, correlation between CAMKK2 expression and overall survival, CAMKK2 in chemotherapy, CAMKK2 in immunotherapy (Fig. 1). After completing the data collection, our study proceeded through several key analyses. Firstly, we discovered that CAMKK2 mutations were associated with prognosis in cancer patients based on genetic alterations. Subsequently, we examined the differences in CAMKK2 expression between tumor and normal tissues at both mRNA and protein levels. Following this, we utilized survival analysis to investigate the relationship between CAMKK2 expression and prognosis in cancer patients. Additionally, we analyzed the correlation between CAMKK2 expression and the dosage of chemotherapeutic agents. Finally, we explored the potential of CAMKK2 as a predictor of immunotherapy efficacy within immunotherapy cohorts.

3.2. Genetic alteration

To comprehensively explore the mutational characteristics of *CAMKK2* during tumor progression, we performed a thorough analysis of mutations and CNVs using genomic data obtained from the TCGA database across various types of cancer. A total of 232 patients exhibited *CAMKK2* gene variants, with 29 patients having both *CAMKK2* mutations and CNVs (Fig. 2A). The largest number of *CAMKK2* variants, as well as the highest mutation rate, were uterine corpus endometrial carcinoma (UCEC) patients (n = 44, ratio = 8.3%), followed by SKCM patients (n = 25, ratio = 5.3%) and OV patients (n = 19, ratio = 4.6%) (Fig. 2A and B). To assess the impact of *CAMKK2* variants on patient prognosis, we performed a comparative analysis with a group of 10,866 patients without *CAMKK2* variants. The results showed that patients with

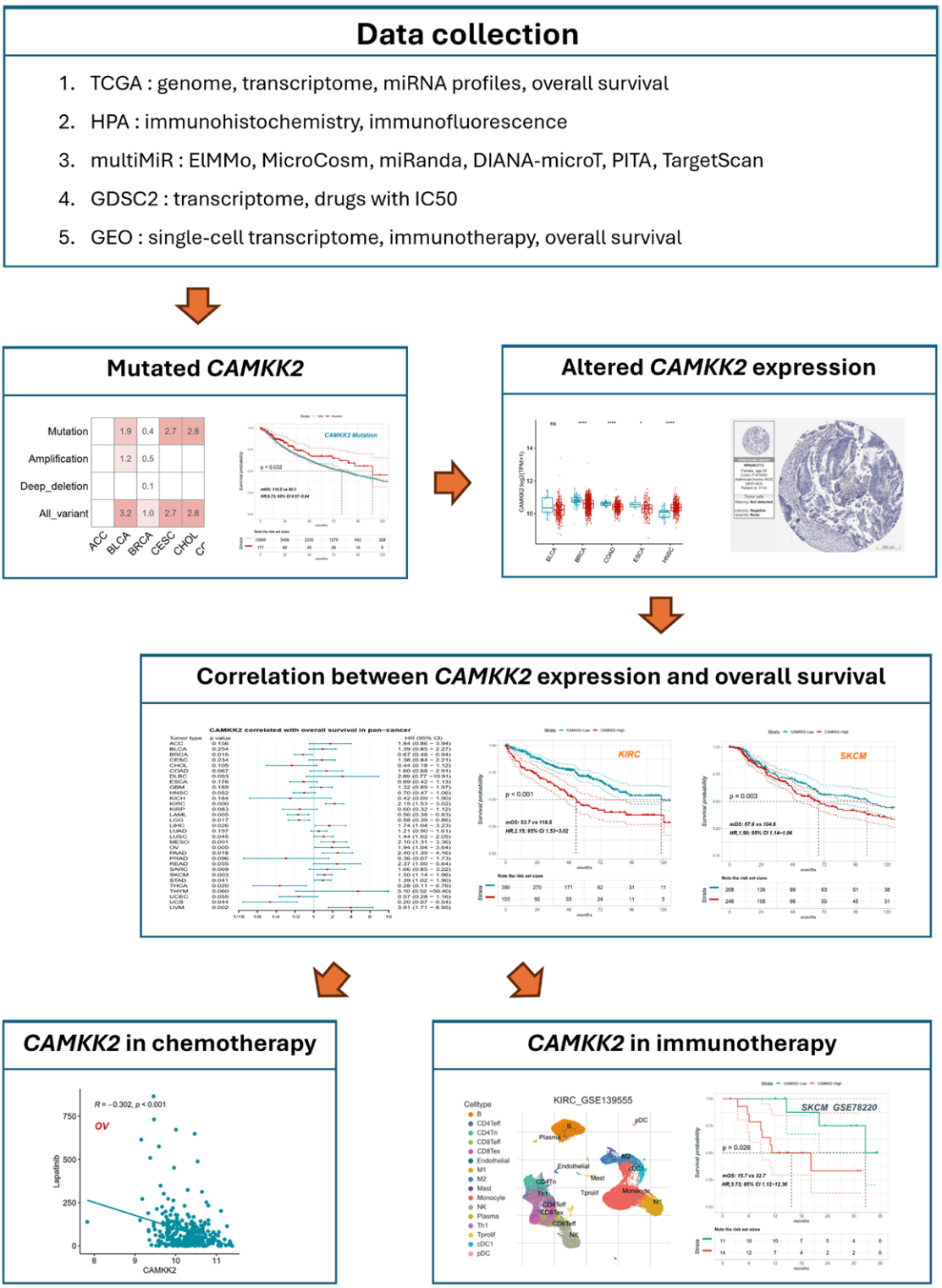

Figure 1. The flow-process diagram of the present study. (A) The research process is divided into 6 main steps, namely data collection, mutated CAMKK2, altered CAMKK2 expression, correlation between CAMKK2 expression and overall survival, CAMKK2 in chemotherapy, CAMKK2 in immunotherapy.

CAMKK2 mutations (n = 177) exhibited a significantly better overall survival prognosis across different types of cancer (P = .032; HR = 0.73, 95% CI 0.57–0.94) (Fig. 2C). However, when comparing patients with *CAMKK2* copy number amplification (n = 65) or deletion (n = 16) to those with wild-type *CAMKK2*, no significant differences in overall survival prognosis were observed (Fig. 2D and E).

3.3. Expression of CAMKK2

A gene expression landscape of *CAMKK2* across cancers was conducted. The analysis revealed that *CAMKK2* exhibited relatively high expression levels in almost all cancer types, as indicated by the large TPM values. Notably, the most significant expression of *CAMKK2* was observed in patients with prostate adenocarcinoma (PRAD) (Fig. 3A). Furthermore, significant

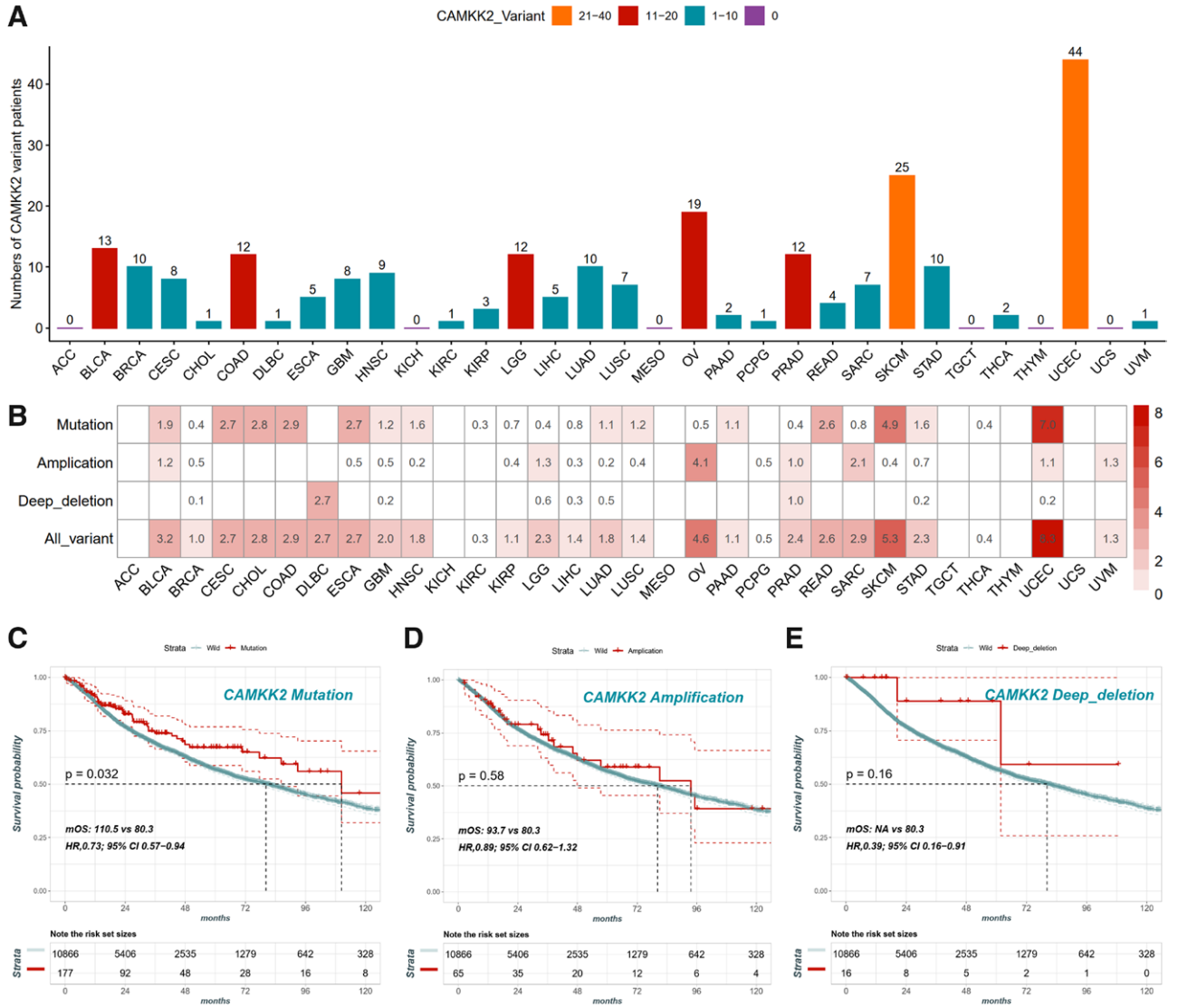

Figure 2. Genetic alterations of *CAMKK2* with implication in prognosis. (A) Number of patients with *CAMKK2* variants, including mutation and copy number amplification or deep deletion, in 32 cancers from the TCGA dataset. (B) The percentage of *CAMKK2* mutation, copy number amplification, deep deletion and all variants in different cancers. (C) Kaplan–Meier (KM) curve of OS analysis between patients with *CAMKK2* mutation and wild in pan-cancer. (D) KM curve of OS analysis between patients with *CAMKK2* amplification and wild in pan-cancer. (E) Curve of OS analysis between patients with *CAMKK2* deep deletion and wild in pan-cancer.

differences in *CAMKK2* transcriptional levels were observed between tumor tissues and their corresponding adjacent normal tissues in thirteen types of cancer, as illustrated in Figure 3B. Specifically, in breast invasive carcinoma (BRCA), colon adenocarcinoma, esophageal carcinoma, lung adenocarcinoma, lung squamous cell carcinoma (LUSC), rectum adenocarcinoma, thyroid carcinoma (THCA), and UCEC, a significant decrease in *CAMKK2* expression was observed in tumor tissues compared to adjacent normal tissues. Conversely, in head and neck squamous cell carcinoma, kidney chromophobe, KIRC, kidney renal papillary cell carcinoma, and PRAD, increased expression of *CAMKK2* was observed in tumor tissues compared to adjacent normal tissues.

3.4. Expression of CAMKK2 protein

Consistent with the mRNA expression levels of *CAMKK2*, immunohistochemical staining results demonstrated weak or undetectable expression of *CAMKK2* protein in tumor cells of BRCA, colon adenocarcinoma, lung adenocarcinoma and LUSC (Fig. 4A–D). Immunohistochemical staining was performed to visualize *CAMKK2* protein expression levels in different tissues. The representative staining results showed varying levels of *CAMKK2* expression in breast (medium), colon (low), lung (low), prostate (high), and kidney (medium) tissues (Fig. 4A–F). Specifically, in prostate tissue (Fig. 4E), *CAMKK2* protein was observed to be highly expressed in both glandular cells and tumor cells. In kidney tissue (Fig. 4F), *CAMKK2* protein was undetectable in cells of the glomeruli, exhibited medium levels in cells of the tubules, and displayed medium levels in tumor cells of renal cancer. Additionally, immunofluorescence reveals that *CAMKK2* is localized to microtubules in 3 tumor cell lines, A-431, U-251MG, and U2OS (Fig. 5).

3.5. Prognostic biomarker

In our comprehensive analysis of the relationship between *CAMKK2* mRNA expression levels and patient survival outcomes, we stratified patients into 2 groups based on *CAMKK2* expression levels within each cancer type. The forest plot

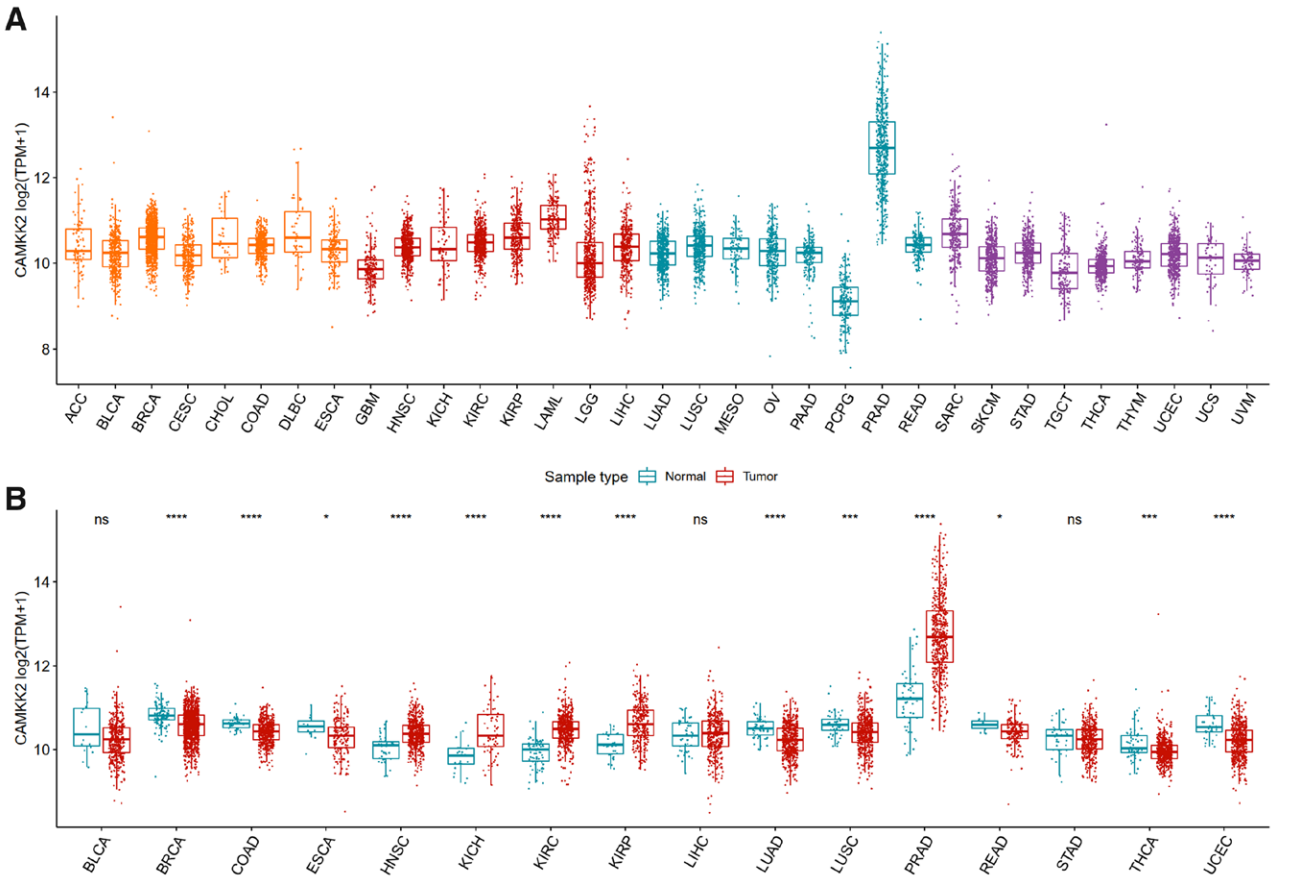

Figure 3. The *CAMKK2* expression status in different tumors and normal tissues. (A) The mRNA expression of *CAMKK2* across 33 cancer types from TCGA data. (B) The TCGA project's *CAMKK2* gene expression difference between tumors and adjacent normal tissues of 16 organs.

(Fig. 6A) illustrates the associations between *CAMKK2* expression and OS across different cancer types. The results revealed that high expression of *CAMKK2* was significantly associated with better OS in BRCA, acute myeloid leukemia, brain lower grade glioma (LGG), THCA, and uterine carcinosarcoma. Conversely, high *CAMKK2* expression was associated with worse OS in KIRC, LIHC, LUSC, mesothelioma (MESO), OV, SKCM, STAD, and uveal melanoma (UVM). To further visualize the impact of *CAMKK2* on patient survival, KM plots were generated for representative cancer types. For BRCA (Fig. 6B) and LGG (Fig. 6C), high *CAMKK2* expression was associated with significantly better OS (BRCA: log-rank $P = .015$, HR = 0.67, 95% CI 0.48–0.94; LGG: log-rank $P = .017$, HR = 0.58, 95% CI 0.39–0.86). Conversely, in KIRC (Fig. 6D), LIHC (Fig. 6E), and KIRC (Fig. 6F), high *CAMKK2* expression was associated with worse OS (KIRC: log-rank $P < .001$, HR = 2.15, 95% CI 1.53–3.02; LIHC: log-rank $P = .026$, HR = 1.74, 95% CI 1.04–3.23; KIRC: log-rank $P = .003$, HR = 1.50, 95% CI 1.14–1.96).

3.6. Targeted miRNA

In our study, we aimed to investigate the microRNA–*CAMKK2* interactions and their role in regulating the physiological activity of *CAMKK2*. To predict microRNAs targeting *CAMKK2*, we utilized 7 databases and identified a total of 728 potential microRNAs (Fig. 7A). Among these, the largest number of microRNAs were predicted by PITA (498) and DIANA-microT (416), followed by ElMMo (378), TargetScan (268), miRanda (140), miRdb (120), and PICTAR (63). Interestingly, 15 microRNAs were predicted by 5 or more of the 7 databases simultaneously. However, when analyzing the TCGA pan-cancer project data, we found that only 13 out of the 728 potential microRNAs targeting *CAMKK2* were detected. These 13 microRNAs were further analyzed for their correlation with *CAMKK2* expression levels. The heatmap (Fig. 7B) shows the correlation between these microRNAs and *CAMKK2* expression across different cancer types. Among them, hsa.miR.129.1.3p showed the strongest positive correlation with *CAMKK2* expression in LGG, and hsa.miR.96.5p showed the strongest negative correlation with *CAMKK2* expression in testicular germ cell tumors.

3.7. Potential drug

We used the Genomics of Drug Sensitivity in Cancer version 2 database to analyze transcriptomic data from 10 tumor cell lines after 161 drug treatments. Using a ridge regression model, we predicted the drug sensitivity of patients from TCGA across 10 cancer types and correlated it with *CAMKK2* expression levels. To identify the drugs with the strongest correlation with *CAMKK2* expression in each tumor type, we selected the top 3 drugs for each cancer, resulting in a heatmap of 26 drugs based on their correlation with *CAMKK2* (Fig. 8A). Among all the analyzed results, the strongest positive correlation between drug sensitivity and *CAMKK2* expression was observed for the drug EPZ004777 in LGG (Fig. 8B). Following that, UMI.77 and NVP.ADW742 showed the next strongest positive correlations with *CAMKK2* in other cancer types (Fig. 8C and D). On the other hand, the most strongly negative correlation between drug sensitivity and *CAMKK2* expression was observed for the drug Lapatinib in OV (Fig. 8E). This was followed by Entinostat in MESO and AZD3759 in OV, both of which also

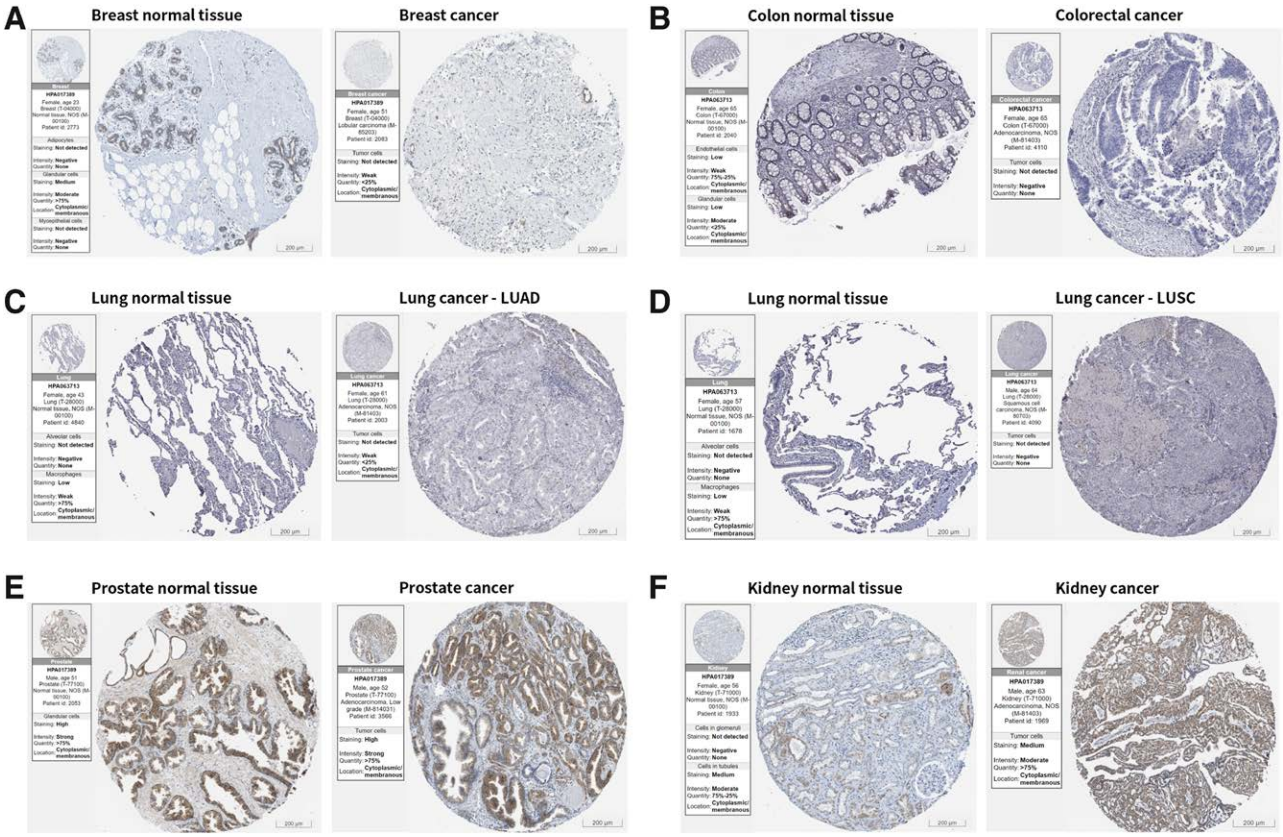

Figure 4. The immunohistochemistry data of *CAMKK2* in tumors and normal tissues of breast (A), colon (B), lung (C and D), prostate (E) and kidney (F) from the human protein atlas.

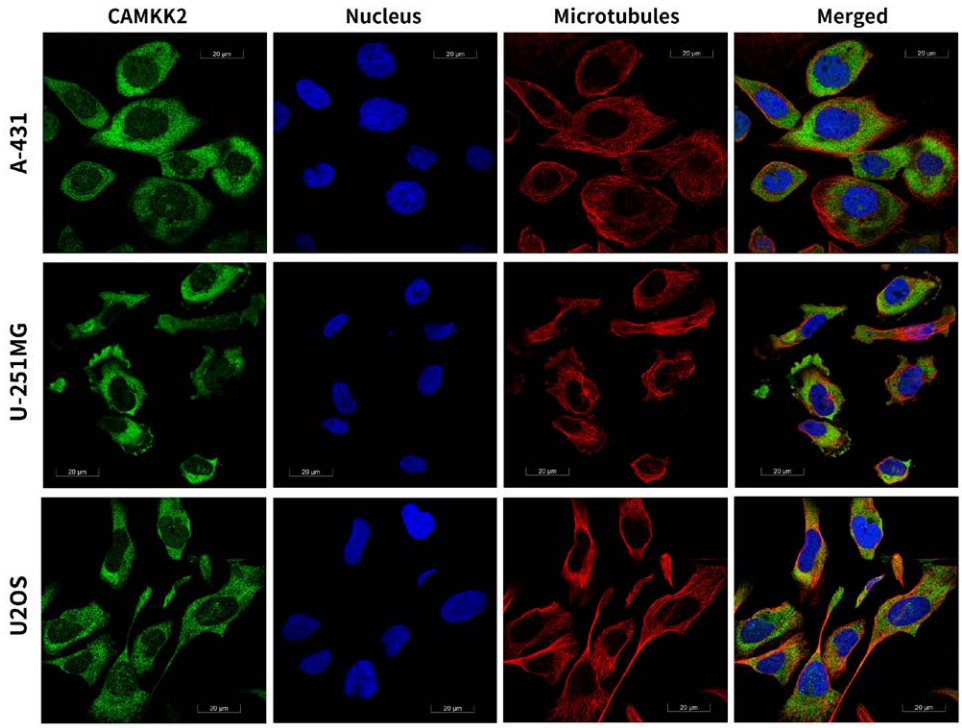

Figure 5. The immunofluorescence data of *CAMKK2* in A-431, U-251MG, and U2OS cell lines from the human protein atlas.

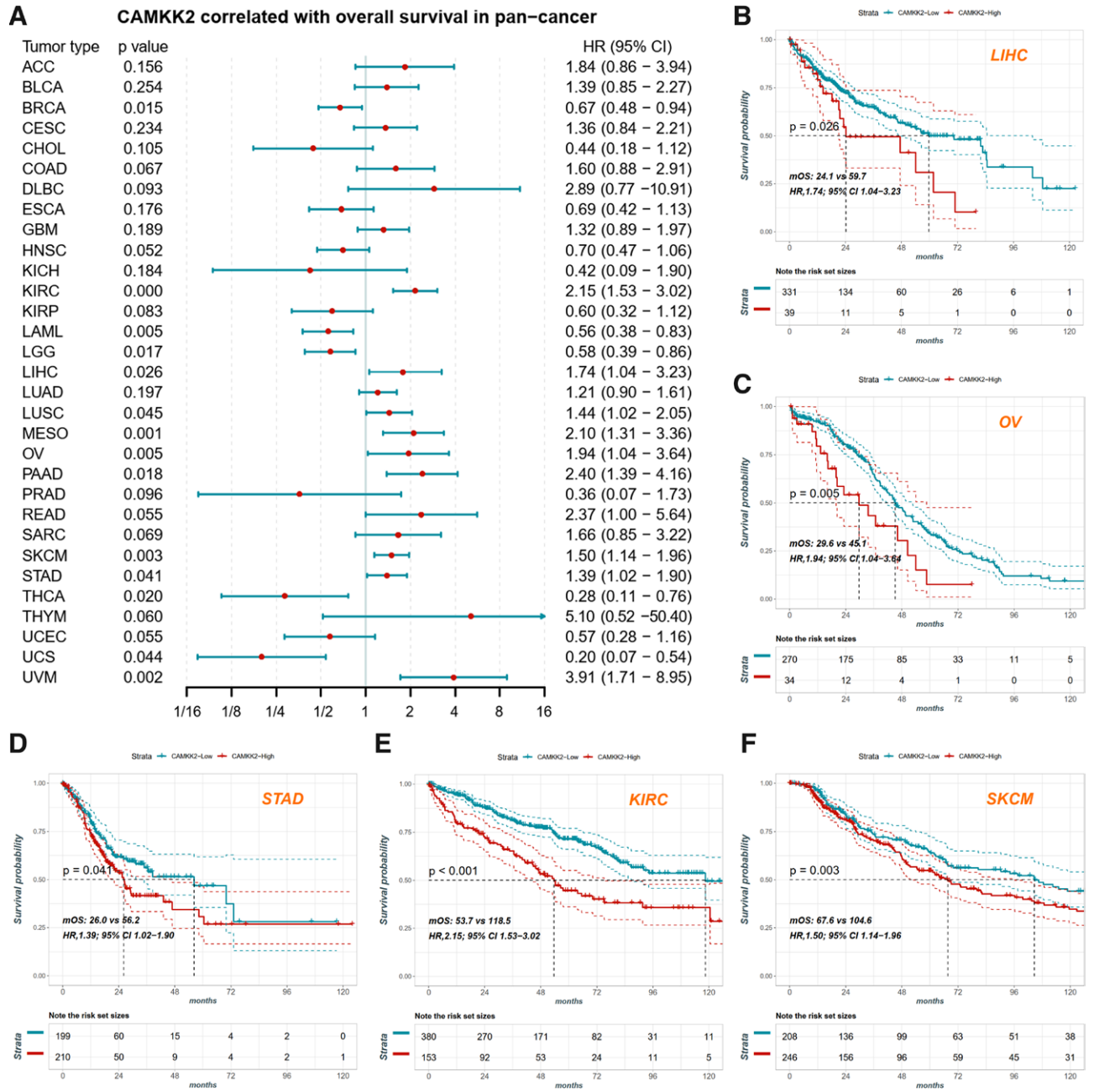

Figure 6. Association of *CAMKK2* with overall survival. (A) Hazard ratio of *CAMKK2* expression in different cancers from the TCGA dataset. (B–F) KM curve of OS analysis of *CAMKK2* in cervical squamous cell carcinoma and endocervical adenocarcinoma (CESC), kidney chromophobe (KICH), LGG, pancreatic adenocarcinoma (PAAD), and UVM in TCGA. The cutoff value of *CAMKK2* in each tumor was performed by surv_cutpoint from the survival package in R language. Red curves mean higher *CAMKK2* expression, and green curves mean lower *CAMKK2* expression.

showed strong negative correlations with *CAMKK2* expression (Fig. 8F and G).

3.8. Single-cell localization

In the analysis of single-cell datasets GSE139555 and GSE145281 in KIRC, we examined the distribution of *CAMKK2* across different cellular taxa. In the GSE139555 dataset, cells were categorized into a total of 16 cell types, including B cell, CD8 + T effector (CD8Teff), macrophage M1, macrophage M2, monocyte, and others (Fig. 9A). Comparing the expression of *CAMKK2* with CD80, a marker of macrophage M2, we observed that *CAMKK2* is mainly expressed in monocytes and macrophage M1 (Fig. 9B and C). This indicates that *CAMKK2* expression is associated with specific immune cell types in the tumor microenvironment of KIRC. A similar cellular expression distribution of *CAMKK2* was also observed in the GSE145281 dataset (Figs. 9D–F), further supporting the consistency of *CAMKK2* expression across different single-cell datasets in KIRC.

3.9. Biomarker for immunotherapy

To evaluate the potential of *CAMKK2* as an immunotherapy biomarker, 6 real-world immunotherapy cohorts were analyzed in this study. In the GSE176307 cohort of BLCA patients, those with low *CAMKK2* expression had a median OS of 6.9 months, which was significantly longer than the 3.4 months observed

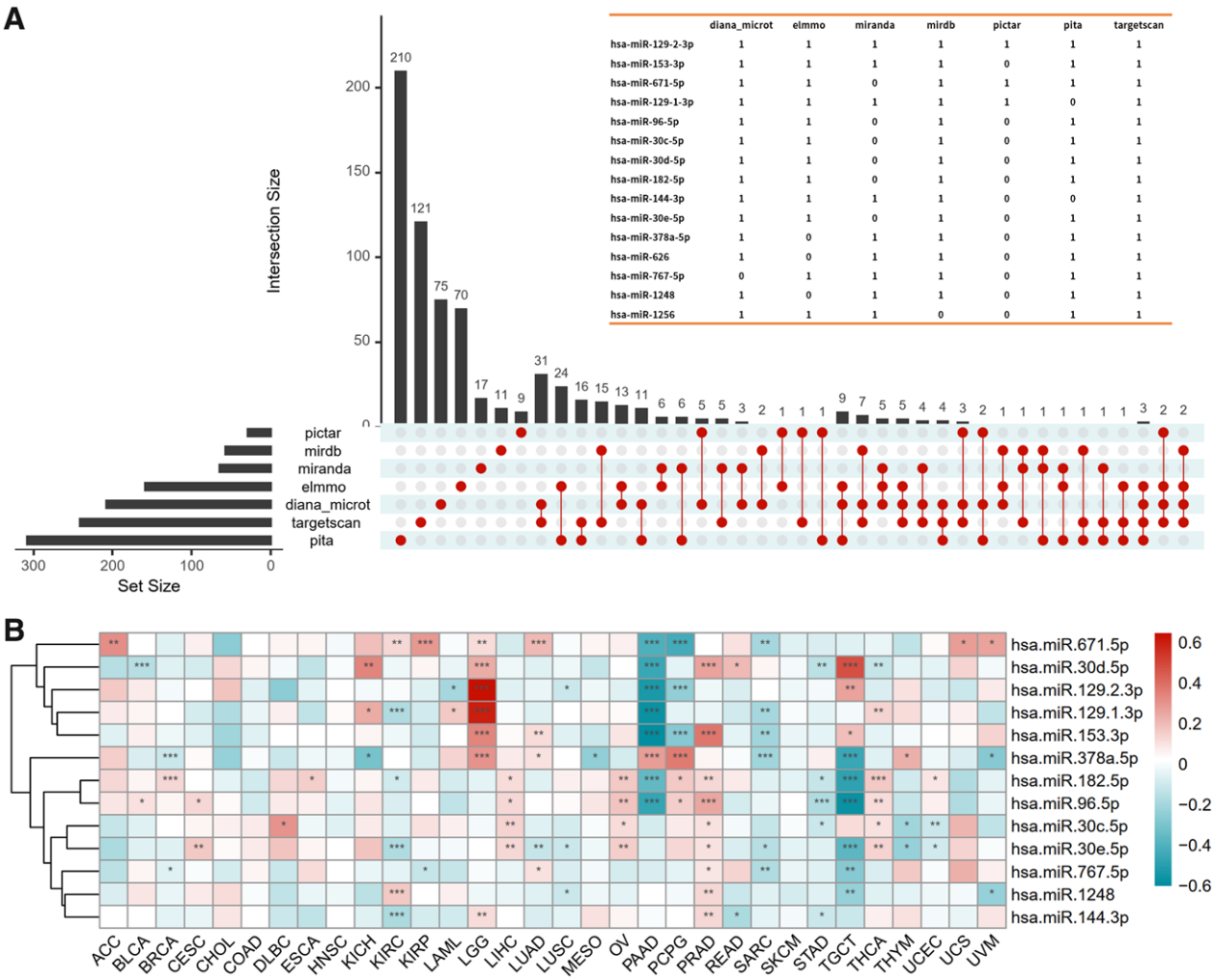

	diana_microt	elmmo	miranda	mirdb	pictar	pita	targetscan
hsa-miR-129-2-3p	1	1	1	1	1	1	1
hsa-miR-153-3p	1	1	1	1	0	1	1
hsa-miR-671-5p	1	1	0	1	1	1	1
hsa-miR-129-1-3p	1	1	1	1	1	0	1
hsa-miR-96-5p	1	1	0	1	0	1	1
hsa-miR-30c-5p	1	1	0	1	0	1	1
hsa-miR-30d-5p	1	1	0	1	0	1	1
hsa-miR-182-5p	1	1	0	1	0	1	1
hsa-miR-144-3p	1	1	1	1	0	0	1
hsa-miR-30e-5p	1	1	0	1	0	1	1
hsa-miR-378a-5p	1	0	1	1	0	1	1
hsa-miR-626	1	0	1	1	0	1	1
hsa-miR-767-5p	0	1	1	1	0	1	1
hsa-miR-1248	1	0	1	1	0	1	1
hsa-miR-1256	1	1	1	0	0	1	1

Figure 7. Potential related miRNAs. (A) The upset plot of *CAMKK2*-targeted miRNAs predicted by 7 mRNA–miRNA databases, of which miRNAs overlapped in more than 3 databases was shown in table. (B) Expression correlation of *CAMKK2* with miRNAs detected in the TCGA project.

in subjects with high *CAMKK2* expression (log-rank $P = .008$; HR = 2.16, 95% CI 1.03–4.56) (Fig. 10A). A similar trend was observed in the BLCA cohort IMvigor210 (Fig. 10B), where patients with lower *CAMKK2* expression had better overall survival compared to those with higher *CAMKK2* expression (log-rank $P = .038$; HR = 1.95, 95% CI 1.19–3.20). This suggests that low *CAMKK2* expression may be associated with an favorable response to immunotherapy in BLCA. In the KIRC cohorts from IMvigor210 and PMID32472114, patients with higher *CAMKK2* expressions seemed to have better overall survival, although the differences did not reach statistical significance in both 2 cohorts (Fig. 10C and D). In the SKCM GSE78220 cohort, patients with higher *CAMKK2* mRNA levels had significantly shorter overall survival compared to patients with lower *CAMKK2* mRNA levels (log-rank $P = .026$; HR = 3.73, 95% CI 1.12–12.36) (Fig. 10E). This indicates that high *CAMKK2* expression may be associated with poorer prognosis in SKCM patients receiving immunotherapy. A similar trend was observed in the GSE91061 cohort, another immunotherapy melanoma cohort, although the difference in overall survival did not reach statistical significance (log-rank $P = .078$; HR = 2.31, 95% CI 0.92–5.85) (Fig. 10F).

4. Discussion

CAMKK2 initially gained recognition for its involvement in facilitating memory formation in the hippocampus and promoting proliferation in prostate tumors.[6,10] However, recent studies have revealed its significant role in diverse cancers and immune cell populations. Nevertheless, current understanding of *CAMKK2*'s impact on different cancer types and immune cell subtypes remains limited. It has been debated that *CAMKK2* mediates proliferation or inhibition in cancer cells, such as its immunosuppression in macrophages and myeloid cells, but antitumor effects in MDSCs and NK cells.[15–18] To bridge this knowledge gap, our study employed a comprehensive multi-omics approach encompassing a wide range of 33 distinct cancer types. To minimize the impact of differences in data processing and statistical methods between different online tools on the results, we downloaded the raw data reported in the literature and wrote R codes for uniform processing. For example, when performing survival analysis for *CAMKK2*, 2 common methods include the cox proportional-hazards model and the KM curve (also known as the Product limit method), whereas our analysis avoids the mixing of the 2 methods used by some online tools. Our objective was to elucidate the molecular mechanisms underlying the observed upregulation of *CAMKK2* in cancer. By exploring *CAMKK2* within the context of cancer and the tumor immune microenvironment, our research not only emphasizes its prognostic significance across diverse cancer types but also unveils its pivotal role in patients undergoing immunotherapy. Through our investigation, we aim to address the intricate relationship between *CAMKK2*, cancer progression, and the tumor immune microenvironment, thereby expanding our comprehension of *CAMKK2*'s functions.

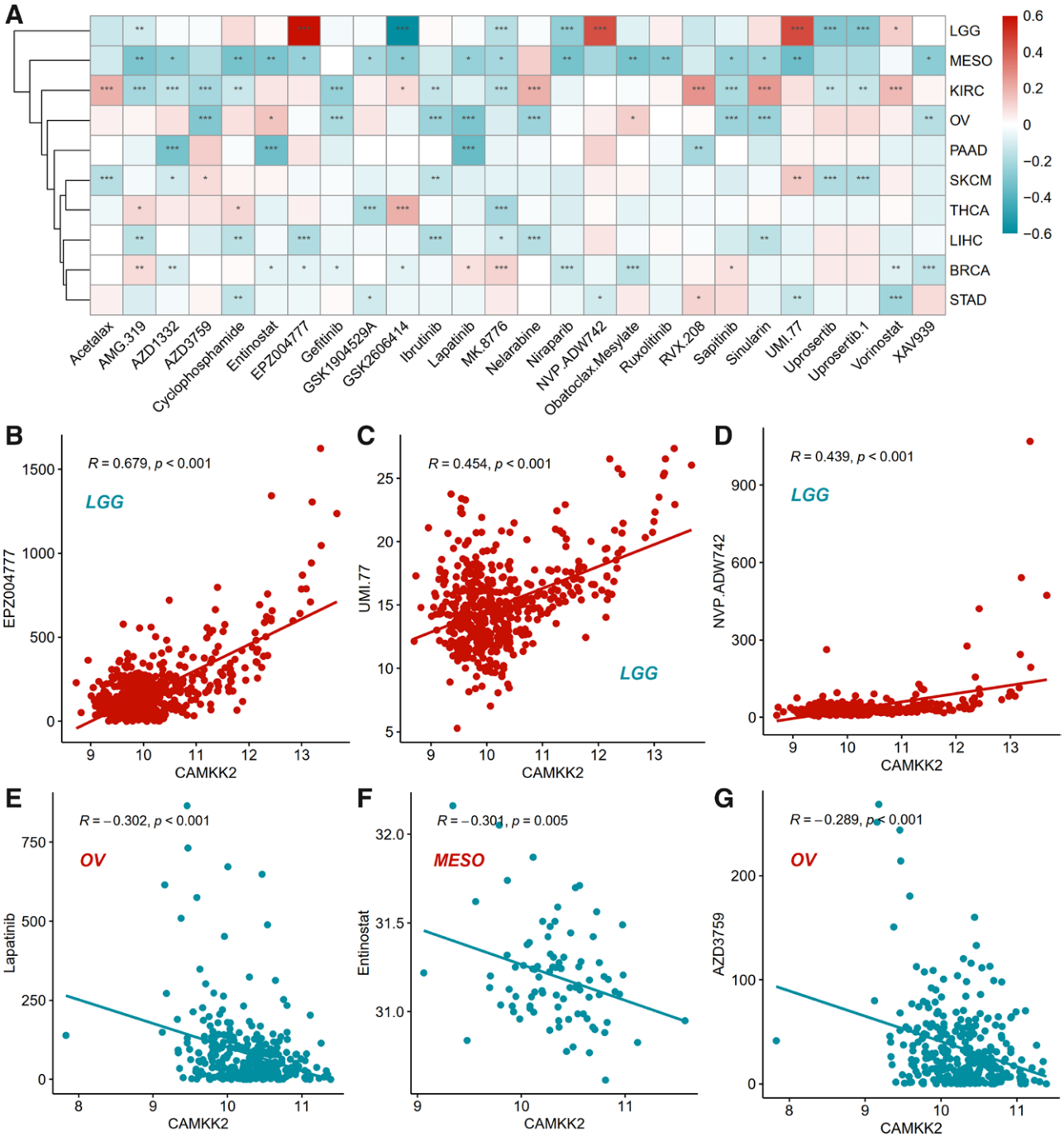

Figure 8. Potential related drugs. (A) Correlation of *CAMKK2* expression with the sensitivity of 26 drugs in pan-cancer by Genomics of Drug Sensitivity in Cancer version 2 GDSC2 data and ridge regression algorithm. The scatter plot of the top positively correlated drug EPZ004777 (B), UMI.77 (C) and NVP. ADW742 (D) in LGG. The scatter plot of the top negatively correlated drug Lapatinib in OV (E), Entinostat in MESO (F) and AZD3759 in OV (G).

Initially, our analysis focused on investigating *CAMKK2* mutations and copy number variations in cancer. This study specifically examines the clinical significance and therapeutic potential of *CAMKK2* as a biomarker in advanced PRAD using various preclinical models.[42–44] Previous research has demonstrated that androgen receptor–*CAMKK2*–AMPK signaling promotes prostate cancer cell growth by enhancing central carbon metabolism, including glucose uptake and phosphorylation.[42,45,46] However, our findings indicate that genetic alterations in *CAMKK2* are only observed in 2.4% of PRAD patients, while the rates are higher in UCEC (8.3%) and OV (4.6%) (Fig. 2B). The increased prevalence of *CAMKK2* variants in UCEC and OV suggests that *CAMKK2* also plays a significant role in the female reproductive system. In OV cell lines HO8910 and OV90, *CAMKK2* has been shown to promote ovarian cancer progression, which is consistent with our findings and hypotheses. Given the higher mutation rate of *CAMKK2* in UCEC, further in vivo and in vitro experiments are warranted to explore its implications.

Then, we analyzed CAMKK2 expression, emphasizing its relationship with overall survival. The subcellular localization of *CAMKK2*, whether in the cytoplasm or nucleus, remains a subject of debate.[43,46–48] However, our immunofluorescence results strongly support cytoplasmic expression of *CAMKK2* (Fig. 5). Previous studies in LIHC, OV, and STAD have suggested that

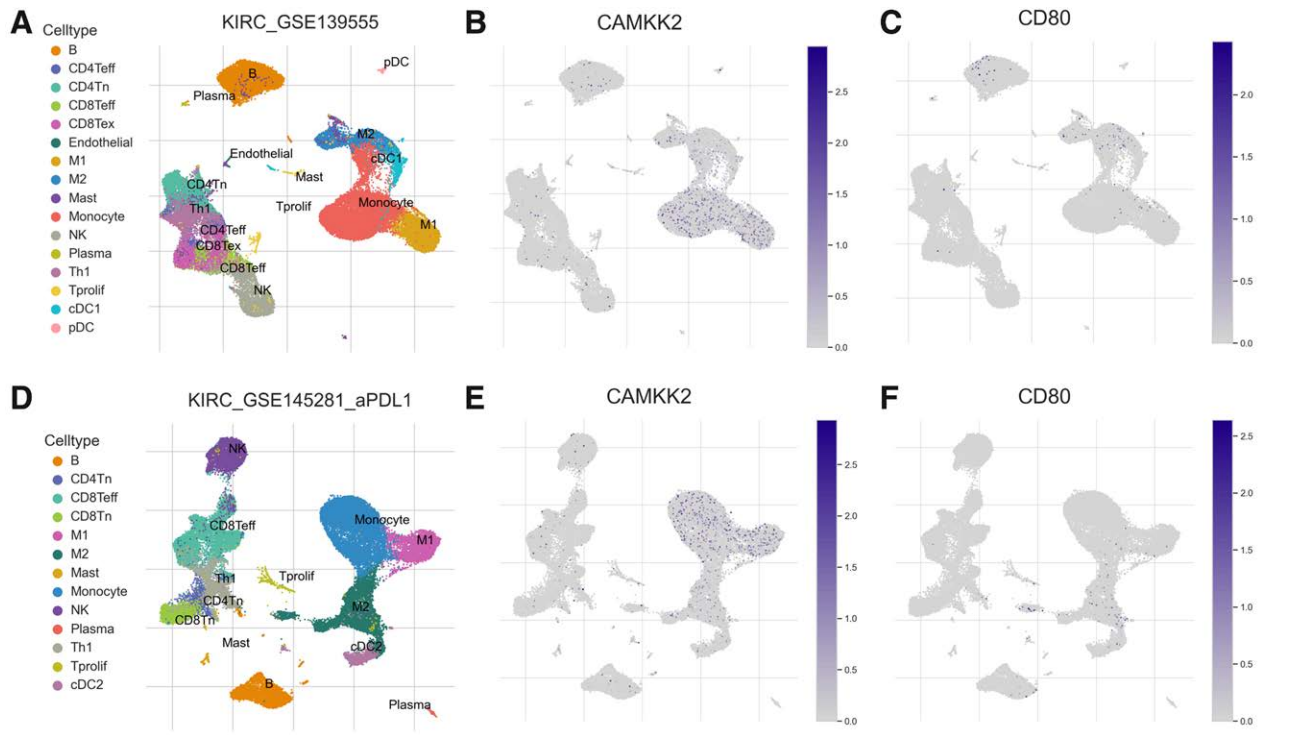

Figure 9. Localizations of *CAMKK2* in single-cell level of KIRC datasets. (A) Cellular taxa of the GSE139555. (B) Distribution of *CAMKK2*. (C) Distribution of *CD80*, as the marker of macrophage M2. (D) Cellular taxa of the GSE145281. (E) Distribution of *CAMKK2*. (F) Distribution of *CD80*.

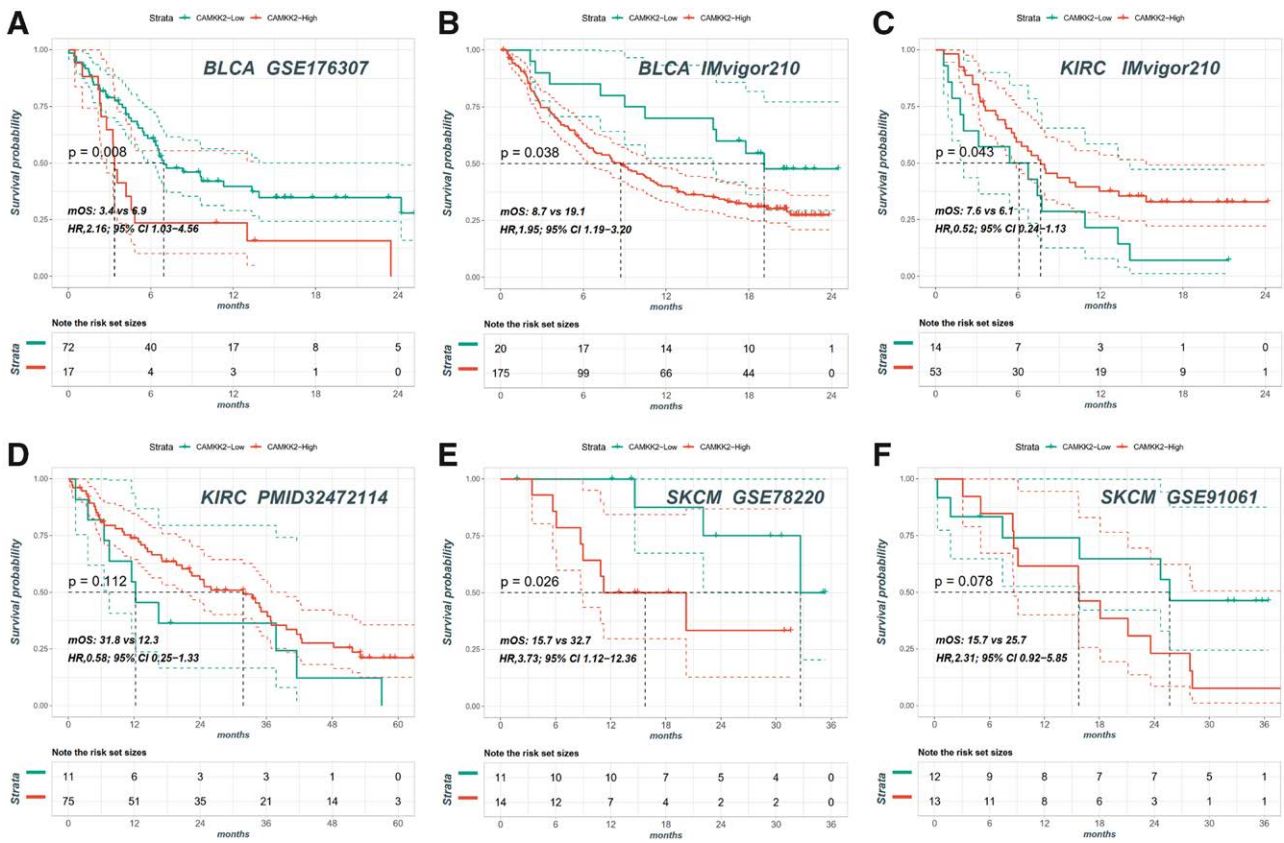

Figure 10. *CAMKK2* as biomarker in patients ongoing immunotherapy. KM curve of OS analysis of *CAMKK2* in BLCA patients from the GSE176307 cohort (A), the IMvigor210 cohort (B). KM curve of OS analysis KIRC patients from the IMvigor210 cohort (C), the PMID32472114 cohort (D). KM curve of OS analysis SKCM patients from the GSE78220 cohort (E), the GSE91061 cohort (F).

elevated *CAMKK2* expression promotes tumor proliferation and metastasis, indicating that patients with high *CAMKK2* expression may have a poorer prognosis.[12,13] However, whether *CAMKK2* can also serve as a prognostic biomarker in other cancers remains unknown. Our survival analysis by KM curve showed that *CAMKK2* also functions as a risk factor in KIRC, LUSC, MESO, SKCM, and UVM (Fig. 6A). Intriguingly, we discovered a favorable role for *CAMKK2* in BRCA, acute myeloid leukemia, LGG, THCA, and uterine carcinosarcoma, which has not been reported previously. Altered *CAMKK2* expression mediated by small-molecule drugs or miRNAs may be a means of clinical intervention to influence patient prognosis. For instance, STO-609, a small-molecule inhibitor of *CAMKK2*, has been shown to inhibit the growth of C4–2B human prostate cancer cells in a castration-resistant prostate cancer xenograft model.[42,49] In our study, we identified a significant positive association between EPZ004777 and *CAMKK2* in LGG (rho = 0.679, $P < .001$) and a significant negative association between Lapatinib and *CAMKK2* in OV (rho = –0.302, $P < .001$) (Fig. 8B and E). Additionally, hsa.miR.129.1.3p and hsa.miR.129.2.3p showed interesting associations with *CAMKK2* in LGG and pancreatic adenocarcinoma (Fig. 7B). It has been reported that miR.129 is involved in tumorigenesis and progression through the regulation of multiple lncRNAs, such as AC130710, MALAT1, and HOTAIR.[50–52] The important role of lncRNA–miRNA–mRNA regulatory network in the tumor microenvironment has been confirmed by more and more studies in recent years.[53–55] With the advancement of interaction prediction studies in computational biology,[56–63] such as GCNCRF and NDALMA,[61,63] it makes lncRNA–miRNA–CAMKK2 also a future research direction that cannot be ignored.

Furthermore, we investigated the involvement of *CAMKK2* in tumor immunity. The specific immune cell types through which *CAMKK2* regulates the tumor microenvironment remain a subject of debate. In skeletal muscle, genetic depletion of Prkaa1, which indirectly inhibits *CAMKK2*, promotes a shift in macrophage polarization from the anti-inflammatory M2 phenotype towards the pro-inflammatory M1-like phenotype. Additionally, dendritic cells derived from Prkaa1-deficient mice exhibit an enhanced inflammatory response to lipopolysaccharide and CD40 stimulation.[64,65] Another study demonstrated that deletion of *CAMKK2* accelerates the terminal differentiation of MDSCs, leading to increased AMPK-dependent production of reactive oxygen species.[17] Furthermore, upregulated *CAMKK2* expression in NK cells has been shown to mitigate the adverse effects of a lactate-rich tumor microenvironment.[18] In our analysis of 2 single-cell datasets, *CAMKK2* was detected in nearly all cell types, with significantly higher expression observed in monocytes and M1 macrophages (Fig. 9). A growing body of research evidence suggests that *CAMKK2* can be involved in the regulation of immune cell infiltration thereby affecting patient immunotherapy. Unfortunately, no studies have been conducted to correlate *CAMKK2* with the efficacy of immunotherapy. Therefore, we collected 6 cohorts of patients with BLCA, KIRC, and SKCM receiving immunotherapy to assess the potential of *CAMKK2* as a biomarker for guiding immunotherapy decisions. As depicted in Figure 10, BLCA and SKCM patients with low *CAMKK2* expression were found to derive benefits from immunotherapy and exhibit improved OS, whereas the opposite trend was observed in KIRC patients. Our study demonstrates for the first time the potential application of *CAMKK2* as a biomarker for the prediction of immunotherapy efficacy.

Despite the comprehensive integration of data from multiple databases in our study, there are several limitations that should be acknowledged. Firstly, the divergent prognostic implications of increased *CAMKK2* expression in different tumor types remain unverified and require further investigation. Secondly, the omics data and patient information utilized in our analysis are derived from publicly available databases and have not been experimentally validated in clinical settings. Therefore, future studies should focus on experimental validations and functional investigations to elucidate the precise role of *CAMKK2* in tumors and immune cells.

In conclusion, our bioinformatics-based pan-cancer analysis of *CAMKK2*, integrating transcriptomic, genomic, pharmacogenomic, and clinical data, has revealed significant associations between *CAMKK2* and both survival prognosis and immune response. Notably, our findings provide novel evidence suggesting that *CAMKK2* may influence the overall survival of BLCA, KIRC, and SKCM patients undergoing immunotherapy through its impact on monocyte and macrophage cells. These insights highlight the potential of combining *CAMKK2* modulators with existing checkpoint inhibitors as a promising therapeutic approach in combating tumors.

Acknowledgments

We thank all the members of this study, especially Senjun Jin for his contribution to the data analysis as a statistician.

Author contributions

Conceptualization: Senjun Jin, Guangzhao Yan.
Data curation: Senjun Jin, Yanyan Wang, Sheng'an Hu, Guangzhao Yan.
Formal analysis: Senjun Jin, Sheng'an Hu.
Investigation: Yanyan Wang.
Project administration: Yanyan Wang, Sheng'an Hu, Guangzhao Yan.
Software: Sheng'an Hu.
Supervision: Guangzhao Yan
Validation: Yanyan Wang, Guangzhao Yan.
Visualization: Senjun Jin, Yanyan Wang.
Writing – original draft: Senjun Jin.
Writing – review & editing: Guangzhao Yan.

References

[1] Rahib L, Wehner MR, Matrisian LM, Nead KT. Estimated projection of US cancer incidence and death to 2040. JAMA Netw Open. 2021;4:e214708.
[2] Mattiuzzi C, Lippi G. Current cancer epidemiology. J Epidemiol Glob Health. 2019;9:217–22.
[3] Siegel RL, Miller KD, Fuchs HE, Jemal A. Cancer statistics, 2021. CA Cancer J Clin. 2021;71:7–33.
[4] Fitzgerald RC, Antoniou AC, Fruk L, Rosenfeld N. The future of early cancer detection. Nat Med. 2022;28:666–77.
[5] Hanahan D. Hallmarks of cancer: new dimensions. Cancer Discov. 2022;12:31–46.
[6] Hsu L-S, Chen G-D, Lee L-S, Chi C-W, Cheng J-F, Chen J-Y. Human Ca2+/calmodulin-dependent protein kinase kinase β gene encodes multiple isoforms that display distinct kinase activity. J Biol Chem. 2001;276:31113–23.
[7] Tokumitsu H, Wayman GA, Muramatsu M, Soderling TR. Calcium/calmodulin-dependent protein kinase kinase: identification of regulatory domains. Biochemistry. 1997;36:12823–7.
[8] Pulliam TL, Goli P, Awad D, Lin C, Wilkenfeld SR, Frigo DE. Regulation and role of CAMKK2 in prostate cancer. Nat Rev Urol. 2022;19:367–80.
[9] Peters M, Mizuno K, Ris L, Angelo M, Godaux E, Giese KP. Loss of Ca2+/calmodulin kinase kinase β affects the formation of some, but not all, types of hippocampus-dependent long-term memory. J Neurosci. 2003;23:9752–60.
[10] Frigo DE, Howe MK, Wittmann BM, et al. CaM kinase kinase β-mediated activation of the growth regulatory kinase AMPK is required for androgen-dependent migration of prostate cancer cells. Cancer Res. 2011;71:528–37.
[11] Chandrasekar T, Yang JC, Gao AC, Evans CP. Mechanisms of resistance in castration-resistant prostate cancer (CRPC). Transl Androl Urol. 2015;4:365–80.
[12] Lin F, Marcelo KL, Rajapakshe K, et al. The camKK2/camKIV relay is an essential regulator of hepatic cancer. Hepatology. 2015;62:505–20.

[13] Najar MA, Modi PK, Ramesh P, et al. Molecular profiling associated with Calcium/Calmodulin-Dependent Protein Kinase Kinase 2 (CAMKK2)-Mediated Carcinogenesis in Gastric Cancer. J Proteome Res. 2021;20:2687–703.
[14] Tomaszewski WH, Waibl-Polania J, Chakraborty M, et al. Neuronal CaMKK2 promotes immunosuppression and checkpoint blockade resistance in glioblastoma. Nat Commun. 2022;13:6483.
[15] Mounier R, Théret M, Arnold L, et al. AMPKα1 regulates macrophage skewing at the time of resolution of inflammation during skeletal muscle regeneration. Cell Metab. 2013;18:251–64.
[16] Racioppi L, Nelson ER, Huang W, et al. CaMKK2 in myeloid cells is a key regulator of the immune-suppressive microenvironment in breast cancer. Nat Commun. 2019;10:2450.
[17] Huang W, Liu Y, Luz A, et al. Calcium/Calmodulin Dependent Protein Kinase Kinase 2 regulates the expansion of tumor-induced myeloid-derived suppressor cells. Front Immunol. 2021;12:754083.
[18] Juras PK, Racioppi L, Mukherjee D, et al. Increased CaMKK2 expression is an adaptive response that maintains the fitness of tumor-infiltrating natural killer cells. Cancer Immunol Res. 2023;11:109–22.
[19] Wang L, Gong Y, Saci A, et al. Fibroblast growth factor receptor 3 alterations and response to PD-1/PD-L1 blockade in patients with metastatic urothelial cancer. Eur Urol. 2019;76:599–603.
[20] Hugo W, Zaretsky JM, Sun L, et al. Genomic and transcriptomic features of response to anti-PD-1 therapy in metastatic melanoma. Cell. 2016;165:35–44.
[21] Riaz N, Havel JJ, Makarov V, et al. Tumor and microenvironment evolution during immunotherapy with nivolumab. Cell. 2017;171:934–49. e16.
[22] Balar AV, Galsky MD, Rosenberg JE, et al. Atezolizumab as first-line treatment in cisplatin-ineligible patients with locally advanced and metastatic urothelial carcinoma: a single-arm, multicentre, phase 2 trial. Lancet. 2017;389:67–76.
[23] Braun DA, Hou Y, Bakouny Z, et al. Interplay of somatic alterations and immune infiltration modulates response to PD-1 blockade in advanced clear cell renal cell carcinoma. Nat Med. 2020;26:909–18.
[24] Yuen KC, Liu LF, Gupta V, et al. High systemic and tumor-associated IL-8 correlates with reduced clinical benefit of PD-L1 blockade. Nat Med. 2020;26:693–8.
[25] Wu TD, Madireddi S, de Almeida PE, et al. Peripheral T cell expansion predicts tumour infiltration and clinical response. Nature. 2020;579:274–8.
[26] Kassambara A, Kassambara MA. Package "ggpubr." R package version 01. 2020;6.
[27] Kolde R, Kolde MR. Package "pheatmap". R package. 2015;1:790.
[28] Therneau TM, Lumley T. Package "survival". R Top Doc. 2015;128:28–33.
[29] Kassambara A, Kosinski M, Biecek P, Fabian S. Package "survminer". Drawing Survival Curves using "ggplot2"(R package version 03 1). 2017;3.
[30] Ponten F, Jirstrom K, Uhlen M. The Human Protein Atlas--a tool for pathology. J Pathol. 2008;216:387–93.
[31] Gordon M, Lumley T, Gordon MM. Package "forestplot". Advanced forest plot using 'grid'graphics. The Comprehensive R Archive Network, Vienna. 2019.
[32] Ru Y, Kechris KJ, Tabakoff B, et al. The multiMiR R package and database: integration of microRNA–target interactions along with their disease and drug associations. Nucleic Acids Res. 2014;42:e133–e133.
[33] Conway JR, Lex A, Gehlenborg N. UpSetR: an R package for the visualization of intersecting sets and their properties. Bioinformatics. 2017;33:2938–40.
[34] Harrell FE Jr, Harrell MFE Jr. Package "hmisc". CRAN2018. 2019;2019:235–236.
[35] Maeser D, Gruener RF, Huang RS. oncoPredict: an R package for predicting in vivo or cancer patient drug response and biomarkers from cell line screening data. Brief Bioinform. 2021;22:bbab260.
[36] Han Y, Wang Y, Dong X, et al. TISCH2: expanded datasets and new tools for single-cell transcriptome analyses of the tumor microenvironment. Nucleic Acids Res. 2023;51:D1425–31.
[37] Gydush G, Nguyen E, Bae JH, et al. Massively parallel enrichment of low-frequency alleles enables duplex sequencing at low depth. Nat Biomed Eng. 2022;6:257–66.
[38] Hao Y, Stuart T, Kowalski MH, et al. Dictionary learning for integrative, multimodal and scalable single-cell analysis. Nat Biotechnol. 2024;42:293–304.
[39] Zhang X, Lan Y, Xu J, et al. CellMarker: a manually curated resource of cell markers in human and mouse. Nucleic Acids Res. 2019;47:D721–8.
[40] Ihaka R, Gentleman R. R: a language for data analysis and graphics. J Comput Graph Stat. 1996;5:299–314.
[41] Allaire J. RStudio: integrated development environment for R. Boston, MA. 2012;770:165–171.
[42] Massie CE, Lynch A, Ramos-Montoya A, et al. The androgen receptor fuels prostate cancer by regulating central metabolism and biosynthesis. EMBO J. 2011;30:2719–33.
[43] Karacosta LG, Foster BA, Azabdaftari G, Feliciano DM, Edelman AM. A regulatory feedback loop between Ca2+/calmodulin-dependent protein kinase kinase 2 (CaMKK2) and the androgen receptor in prostate cancer progression. J Biol Chem. 2012;287:24832–43.
[44] Hurwitz AA, Foster BA, Allison JP, Greenberg NM, Kwon ED. The TRAMP mouse as a model for prostate cancer. Curr Protoc Immunol. 2001;45:20.5.1–20.5.23.
[45] White MA, Tsouko E, Lin C, et al. GLUT12 promotes prostate cancer cell growth and is regulated by androgens and CaMKK2 signaling. Endocr Relat Cancer. 2018;25:453–69.
[46] Karacosta LG, Kuroski LA, Hofmann WA, et al. Nucleoporin 62 and Ca2+/calmodulin dependent kinase kinase 2 regulate androgen receptor activity in castrate resistant prostate cancer cells. Prostate. 2016;76:294–306.
[47] Green MF, Anderson KA, Means AR. Characterization of the CaMKKbeta-AMPK signaling complex. Cell Signal. 2011;23:2005–12.
[48] Sakagami H, Umemiya M, Saito S, Kondo H. Distinct immunohistochemical localization of two isoforms of Ca2+/calmodulin-dependent protein kinase kinases in the adult rat brain. Eur J Neurosci. 2000;12:89–99.
[49] Tokumitsu H, Inuzuka H, Ishikawa Y, Ikeda M, Saji I, Kobayashi R. STO-609, a specific inhibitor of the Ca2+/calmodulin-dependent protein kinase kinase. J Biol Chem. 2002;278:4368–15818.
[50] Xiong Z, Wang L, Wang Q, Yuan Y. Lnc RNA MALAT 1/miR-129 axis promotes glioma tumorigenesis by targeting SOX 2. J Cell Mol Med. 2018;22:3929–40.
[51] Wu Q, Meng WY, Jie Y, Zhao H. LncRNA MALAT1 induces colon cancer development by regulating miR-129-5p/HMGB1 axis. J Cell Physiol. 2018;233:6750–7.
[52] Xu C, Shao Y, Xia T, et al. lncRNA-AC130710 targeting by miR-129-5p is upregulated in gastric cancer and associates with poor prognosis. Tumour Biol. 2014;35:9701–6.
[53] Wang X, Yin H, Zhang L, et al. The construction and analysis of the aberrant lncRNA-miRNA-mRNA network in non-small cell lung cancer. J Thorac Dis. 2019;11:1772–8.
[54] Wang M, Zheng S, Li X, Ding Y, Xu H. Integrated analysis of lncRNA-miRNA-mRNA ceRNA network identified lncRNA EPB41L4A-AS1 as a potential biomarker in non-small cell lung cancer. Front Genet. 2020;11:511676.
[55] Wang P, Li J, Zhao W, et al. A novel LncRNA-miRNA-mRNA triple network identifies LncRNA RP11-363E7. 4 as an important regulator of miRNA and gene expression in gastric Cancer. Cell Physiol Biochem. 2018;47:1025–41.
[56] Chen Z, Zhang L, Sun J, Meng R, Yin S, Zhao Q. DCAMCP: A deep learning model based on capsule network and attention mechanism for molecular carcinogenicity prediction. J Cell Mol Med. 2023;27:3117–26.
[57] Sun F, Sun J, Zhao Q. A deep learning method for predicting metabolite–disease associations via graph neural network. Brief Bioinform. 2022;23:bbac266.
[58] Hu H, Feng Z, Lin H, et al. Gene function and cell surface protein association analysis based on single-cell multiomics data. Comput Biol Med. 2023;157:106733.
[59] Wang T, Sun J, Zhao Q. Investigating cardiotoxicity related with hERG channel blockers using molecular fingerprints and graph attention mechanism. Comput Biol Med. 2023;153:106464.
[60] Gao H, Sun J, Wang Y, et al. Predicting metabolite–disease associations based on auto-encoder and non-negative matrix factorization. Brief Bioinform. 2023;24:bbad259.
[61] Wang W, Zhang L, Sun J, Zhao Q, Shuai J. Predicting the potential human lncRNA–miRNA interactions based on graph convolution network with conditional random field. Brief Bioinform. 2022;23:bbac463.
[62] Meng R, Yin S, Sun J, Hu H, Zhao Q. scAAGA: Single cell data analysis framework using asymmetric autoencoder with gene attention. Comput Biol Med. 2023;165:107414.
[63] Zhang L, Yang P, Feng H, Zhao Q, Liu H. Using network distance analysis to predict lncRNA–miRNA interactions. Interdiscip Sci. 2021;13:535–45.
[64] Carroll KC, Viollet B, Suttles J. AMPKalpha1 deficiency amplifies proinflammatory myeloid APC activity and CD40 signaling. J Leukoc Biol. 2013;94:1113–21.
[65] Wang X, Quinn PJ. Lipopolysaccharide: biosynthetic pathway and structure modification. Prog Lipid Res. 2010;49:97–107.